Nanoscale Res Lett (2009) 4:809–813
DOI 10.1007/s11671-009-9319-5

NANO EXPRESS

Enhanced Luminescence of Eu-Doped TiO_2 Nanodots

Ming Luo · Kui Cheng · Wenjian Weng · Chenlu Song · Piyi Du · Ge Shen · Gang Xu · Gaorong Han

Received: 19 February 2009 / Accepted: 6 April 2009 / Published online: 25 April 2009
© to the authors 2009

Abstract Monodisperse and spherical Eu-doped TiO_2 nanodots were prepared on substrate by phase-separation-induced self-assembly. The average diameters of the nanodots can be 50 and 70 nm by changing the preparation condition. The calcined nanodots consist of an amorphous TiO_2 matrix with Eu^{3+} ions highly dispersed in it. The Eu-doped TiO_2 nanodots exhibit intense luminescence due to effective energy transfer from amorphous TiO_2 matrix to Eu^{3+} ions. The luminescence intensity is about 12.5 times of that of Eu-doped TiO_2 film and the luminescence lifetime can be as long as 960 μs.

Keywords TiO_2 · Eu^{3+} · Nanodots · Phase-separation-induced self-assembly · Luminescence

Introduction

It is well-known that rare earth (RE) ions can exhibit rich spectral properties [1–4]. The direct excitation of the RE ions is inefficient because of parity-forbidden f–f transitions. Therefore, host materials are required to excite the RE ions efficiently in a wide spectral range for realizing their full potential in optoelectronic devices and flat panel displays [5, 6]. For these applications, inorganic oxide materials exhibit superior advantages in terms of their good chemical, thermal, and mechanical properties [7–9]. For example, Y_2O_3:Eu is one red emitting phosphor compound commonly used [7, 10–12]. However, high costs prevent its further developments. As one of the recently developed alternative oxide host materials, titanium oxide (TiO_2) is demonstrated to be a good sensitizer to absorb light and transfer energy to Eu^{3+} ions [4, 8, 13–16]. It also has advantages in practical applications because of its low cost, chemical and thermal stability, and good mechanical properties [17]. However, the Eu–Eu interaction in TiO_2 matrix may greatly decrease the luminescence intensity. It has been demonstrated that TiO_2 amorphous region is an ideal framework for Eu^{3+} ions by significantly decreasing the non-desired Eu–Eu interaction [8, 14, 16]. Moreover, monodisperse spherical and small phosphor particles prepared on a substrate are greatly demanded not only for improvement of luminescence performance and screen resolution, but also for technological applications, such as light emitting devices and flat panel displays.

In our previous work, we have developed a novel method, i.e., phase-separation-induced self-assembly, to synthesize monodisperse polycrystalline TiO_2 nanodots on substrate (unpublished). The TiO_2 nanodot was found to be composed of many small nanocrystallites embedded in amorphous surrounding, which could be an ideal host matrix for Eu^{3+} ions. In the present study, monodisperse and spherical Eu-doped TiO_2 nanodots were successfully prepared on substrate via the facile approach. The size of the Eu-doped TiO_2 nanodots can be controlled by varying the preparation condition. The Eu-doped TiO_2 nanodots exhibited intense sharp luminescence under ultraviolet excitation. The luminescence intensity could be 12.5 times as strong as Eu-doped TiO_2 film with the luminescence lifetime to be 960 μs.

M. Luo · K. Cheng · W. Weng (✉) · C. Song · P. Du · G. Shen · G. Xu · G. Han
Department of Material Science and Engineering, State Key Laboratory of Silicon Materials, Zhejiang University, Hangzhou 310027, People's Republic of China
e-mail: wengwj@zju.edu.cn

Experimental

The precursor sol for Eu-doped TiO_2 nanodots is similar with that of film prepared by the sol–gel spin-coating method except for the addition of polyvinyl pyrrolidone (PVP) acting as both an initiator to induce the phase separation and a counterpart phase. The detailed preparation procedures are described as follows. A certain amount of Tris (2,2,6,6-tetramethyl-3,5-heptanedionato) europium [$Eu(TMHD)_3$] was initially dissolved into pure ethanol (ETOH). After stirring for some time, acetylacetone (AcAc), distilled water (H_2O), and titanium tetrabutoxide (TBOT) were added to the above solution with stirring to yield a mol ratio of $Eu(TMHD)_3$:AcAc:TBOT:H_2O to be 0.1:0.3:1:1. Then, PVP was added into above solution to obtain the homogeneous precursor sol. Samples were prepared by spin-coating the precursor sols on silicon substrates at 8000 rpm speed for 40 s, followed by calcining in air at 500 °C for 2 h in a muffle furnace. The preparation of film sample follows the above procedures except not to add PVP in the precursor sol. Detailed preparation conditions and morphology features of samples are listed in Table 1. Scanning electron microscope (SEM) imaging was performed on a HITACHI S-4800 microscope to investigate the morphology of the Eu-doped TiO_2 nanodots. The nanodot structure was observed using a transmission electron microscope (TEM) (JEOL, JEM-2010). The chemical composition of the sample was determined by energy dispersive X-ray spectroscopy (EDS) attached on the TEM. The room-temperature photoluminescence (PL) spectra and the lifetime curves were recorded on a steady-state/lifetime spectrofluorometer (FLS920) using a Xe lamp as the excitation source.

Results and Discussion

The formation mechanism of the Eu-doped TiO_2 nanodots by the phase-separation-induced self-assembly is based on Marangoni effect [18–20]. After the precursor sol is spin-coated on the substrate, the ethanol in the liquid film is evaporated but the evaporation rate is gradient in thickness direction. The Marangoni effect can lead to convective flows in the liquid film with a large temperature gradient during the spin-coating process. The requirement of minimizing the extra surface free energy induces the formations of the TBOT/$Eu(TMHD)_3$ droplets and the PVP phase. After hydrolysis, the TBOT/$Eu(TMHD)_3$ droplets become gel nanodots, which form Eu-doped TiO_2 nanodots after calcination.

Table 1 Preparation conditions and morphology features of different samples

Sample	TBOT (mol/L)	PVP (g/L)	Diameter/thickness (nm)	Density ($\times 10^{10}$ cm^{-2})
Nanodot-1	0.08	50	50	1.8
Nanodot-2	0.1	50	70	1.0
Film	0.1	–	20	–

Figure 1 shows the SEM images and the corresponding size distribution histograms of the Eu-doped TiO_2 nanodots (contain 10 mol% Eu^{3+}) on silicon substrates after calcining at 500 °C. They illustrate that the Eu-doped TiO_2 nanodots are well-dispersed and have spherical shape. The average sizes of nanodots are 50 and 70 nm in diameter for nanodot-1 and nanodot-2, respectively. Clearly, the increase of the concentration of TBOT in the precursor sol (from 0.08 to 0.1 M) will induce the formation of larger nanodots as a result of the mass accumulation of TBOT droplets. It is confirmed that the size of the Eu-doped TiO_2 nanodots can be finely controlled by changing the TBOT concentration.

Figure 2a–c present the TEM and the high-resolution TEM (HRTEM) images of the Eu-doped TiO_2 nanodots. The spherical nanodot shape determined by the TEM is in a good agreement with that displayed in the SEM images. From the TEM images, the nanodots have a rough surface, they are suggested to be dense because they have undergone a heat-treatment at 500 °C for a long time of 2 h. The existence of Eu is confirmed by the EDS spectrum shown in Fig. 2d. The Cu element comes from the coating of the grid for TEM measurement. The selected-area electron diffraction pattern (inset of Fig. 2b) illustrates that the nanodots are amorphous, indicating that Eu^{3+} doping in TiO_2 nanodots significantly depresses the nucleation and the growth of the TiO_2 crystallites.

Under UV light excitation at wavelength of 300 nm, the Eu-doped TiO_2 nanodots display strong red light luminescence. The PL spectra of Eu-doped TiO_2 nanodots and film are shown in Fig. 3. The luminescence peaks are associated to the Eu^{3+} f–f transitions from $^5D_0$ level to ^7F_J ground level. The strongest emission centered at 614 nm is attributed to the forced electric dipole transition ($^5D_0 \rightarrow {}^7F_2$), which is allowed if the Eu^{3+} ions occupies a site without an inverse center. The second strongest emission peak (592 nm) is due to the allowed magnetic dipole transition ($^5D_0 \rightarrow {}^7F_1$). Other weak bands centered at 579, 654, and 702 nm correspond to the $^5D_0 \rightarrow {}^7F_0$, $^5D_0 \rightarrow {}^7F_3$, and $^5D_0 \rightarrow {}^7F_4$ transitions of Eu^{3+} ions, respectively. Inhomogeneous broadening of some luminescence bands can be attributed to the fact that the Eu^{3+} ions are distributed in an amorphous oxide environment [8].

The intensities of the emission peak at 614 nm of Eu-doped TiO_2 nanodots show significant increase compared with the Eu-doped TiO_2 film. The intensity ratio per unit mass of film, nanodot-1 and nanodot-2 is 1:6.4:12.5. The

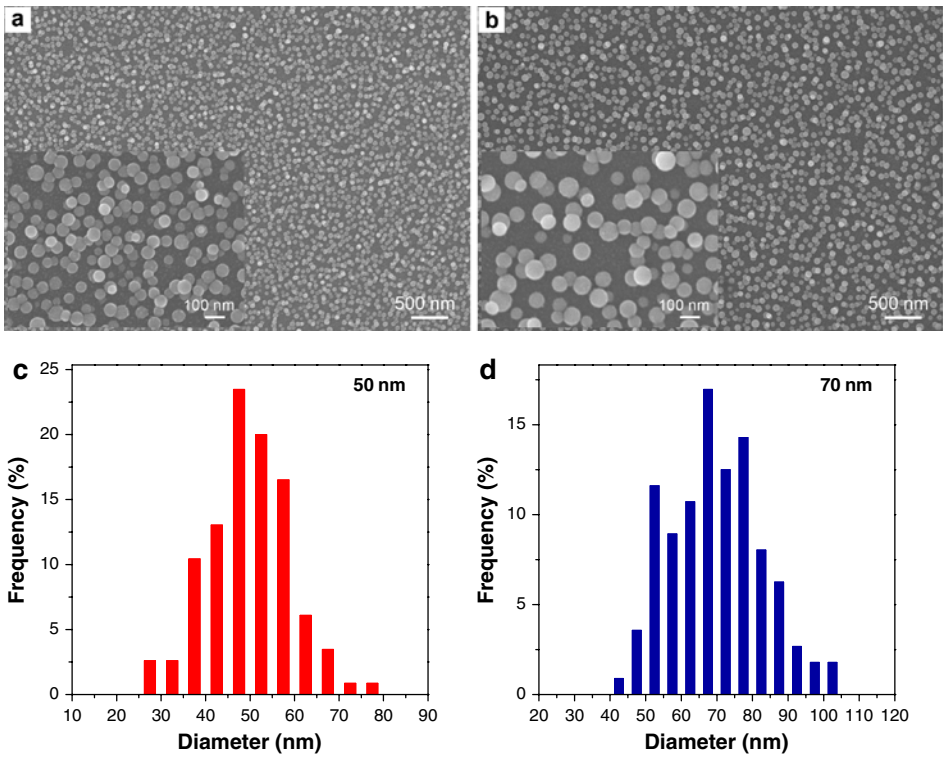

Fig. 1 **a**, **b** SEM images of Eu-doped TiO_2 nanodots on silicon substrates after calcining at 500 °C and **c**, **d** the corresponding size distribution histograms (**a**, **c**: nanodot-1; **b**, **d**: nanodot-2)

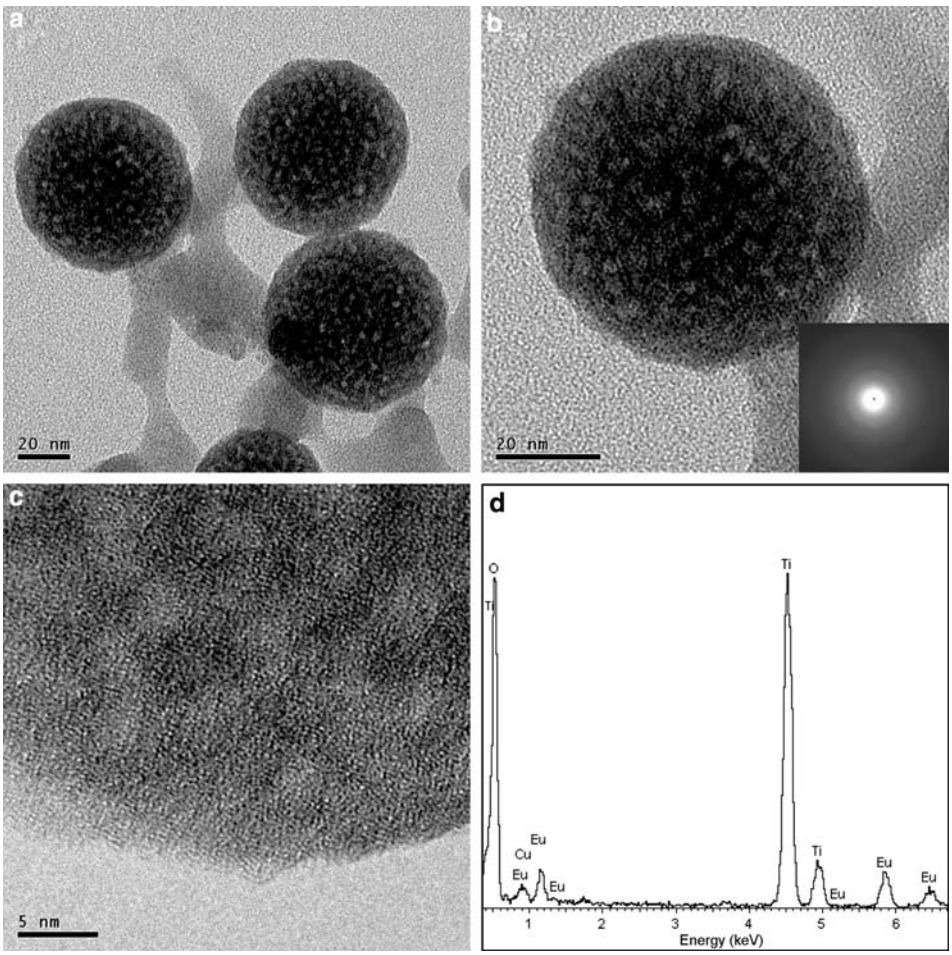

Fig. 2 TEM images (**a**, **b**), HRTEM images (**c**), and EDS spectrum (**d**) of Eu-doped TiO_2 nanodots (500 °C calcination)

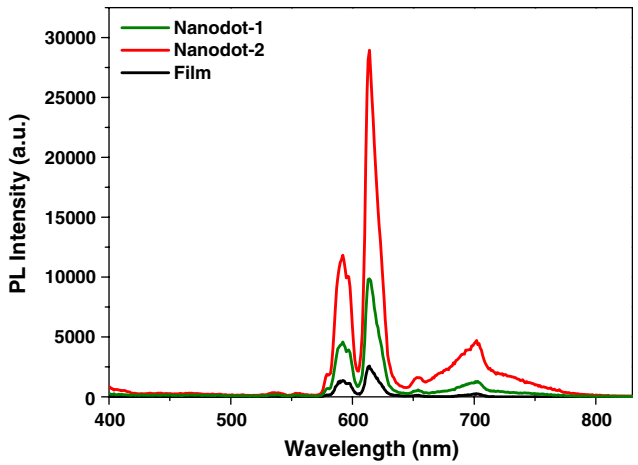

Fig. 3 PL spectra of Eu-doped TiO_2 nanodots and film

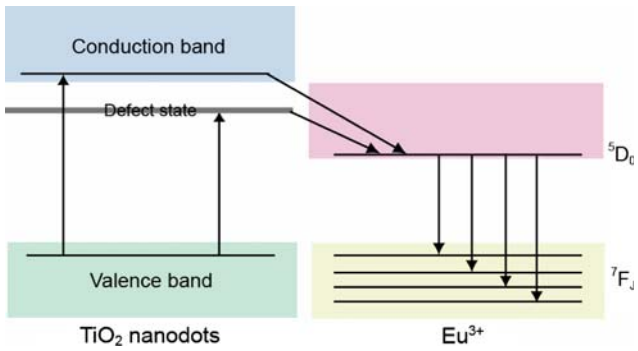

Fig. 4 A scheme of energy transfer for Eu-doped TiO_2 nanodots

enhanced luminescence of Eu-doped TiO_2 nanodots are brought about by their unique structure and morphology. In Eu-doped TiO_2 nanodots, the amorphous TiO_2 host matrix not only provides an ideal host for well-dispersed and highly accommodated concentration Eu^{3+} ions, but also functions as good sensitizer to efficiently absorb light and transfer energy to Eu^{3+} ions [8, 14, 16]. This energy transfer process can be illustrated in the schematic model in Fig. 4. Electrons are initially excited to both of the conduction band and the defect states of TiO_2 after absorbing light. Since the energy levels of conduction band and defect state are higher than that of the emitting state ($^5D_0$) of Eu^{3+} ions, energy transfer to the Eu^{3+} crystal-field states then occurs, resulting in efficient luminescence. Moreover, the improved PL performance of nanodot samples also results from the reduced internal reflection by forming rougher surface, i.e., well-dispersed nanodots on substrate [10, 11]. It is also noted that there is an obvious decrease of luminescence intensity for nanodot-1 compared with nanodot-2. This could be because smaller nanodots have more defects, acting as the non-radiative recombination centers.

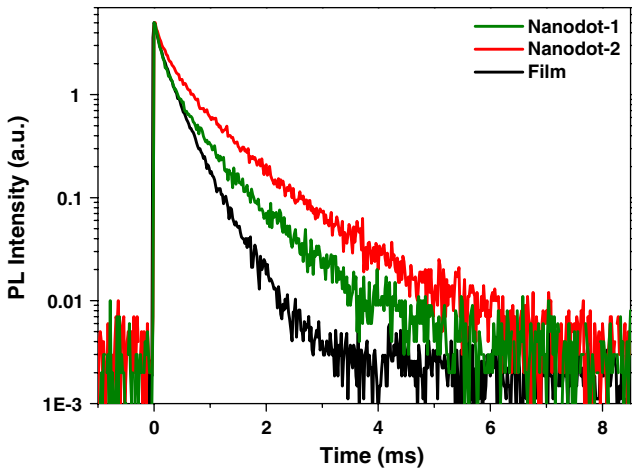

Fig. 5 Lifetime spectra of Eu-doped TiO_2 nanodots and film

To further study the luminescence process of Eu-doped TiO_2 nanodots, PL lifetime was measured under excitation wavelength of 300 nm by monitoring the emission peak at 614 nm ($^5D_0 \rightarrow {}^7F_2$). The measured lifetime spectra are shown in Fig. 5. The lifetime curves of Eu-doped TiO_2 nanodots decay much slower than that of Eu-doped TiO_2 film, indicating a significant lifetime increase for nanodot samples. By using a biexponential function, reasonable fits of the decay curves are obtained. The long-lived components with lifetime of all samples are determined to be 750 (nanodot-1), 960 (nanodot-2), and 450 μs (film). Additionally, short-lived components with lifetime of 150 (nanodot-1), 260 (nanodot-2), and 80 μs (film) were also detected. The long component is typical for the $^5D_0 \rightarrow {}^7F_2$ transition of Eu^{3+}, while the short component is attributed to the weak intrinsic luminescence from the defect states of TiO_2 [21–23]. It can be concluded that the lifetimes for $^5D_0 \rightarrow {}^7F_2$ transition of Eu^{3+} in nanodot-1 and nanodot-2 are 750 and 960 μs, which are longer than the reported lifetime values for Eu-doped TiO_2 nanocrystals [15], nanotubes [15], and mesostructured films [8]. We consider that the amorphous TiO_2 matrix can provide a fine surrounding to prevent from the quenching of the Eu^{3+} $^5D_0 \rightarrow {}^7F_2$ luminescence, which is responsible for the long PL lifetime of the Eu-doped TiO_2 nanodots.

Conclusion

In this work, monodisperse Eu-doped TiO_2 nanodots with spherical shape were successfully synthesized on substrate by utilizing the phase-separation-induced self-assembly during the spin-coating process. The size of the Eu-doped TiO_2 nanodots can be controlled by changing the preparation condition. The average diameter of nanodots reduces

from 70 to 50 nm if the TBOT concentration in the precursor sol decreases from 0.1 to 0.08 M. After calcining at 500 °C, the Eu-doped TiO_2 nanodots remain amorphous with the Eu^{3+} ions well-dispersed in the amorphous TiO_2 matrix. The amorphous TiO_2 framework acts as an effective sensitizer to absorb light and transfer energy to Eu^{3+} ions, resulting in strong luminescence from Eu^{3+} ions. The PL intensity of Eu-doped TiO_2 nanodots (nanodot-1) can be 12.5 times as strong as film, and the PL lifetime is determined to be as long as 960 μs. It is believed that the good luminescence properties endow the Eu-doped TiO_2 nanodots with potentials in many fields, such as light emitting devices, flat panel displays, etc.

Acknowledgment This work was supported by the Nature Science Foundation of China (Grant no. 50572093, 30870627).

References

1. J.H. Van Vleck, J. Phys. Chem. **41**, 67 (1937). doi:10.1021/j150379a006
2. B.R. Judd, Phys. Rev. **127**, 750 (1962). doi:10.1103/PhysRev.127.750
3. E. Danielson, M. Devenney, D.M. Giaquinta, J.H. Golden, R.C. Haushalter, E.W. McFarland, D.M. Poojary, C.M. Reaves, W.H. Weinberg, X.D. Wu, Science **279**, 837 (1998). doi:10.1126/science.279.5352.837
4. A. Conde-Gallardo, M. García-Rocha, I. Hemández-Calderón, R. Palomino-Merino, Appl. Phys. Lett. **78**, 3436 (2001). doi:10.1063/1.1372338
5. J. Kido, Y. Okamoto, Chem. Rev. **102**, 2357 (2002). doi:10.1021/cr010448y
6. L. Ozawa, M. Itoh, Chem. Rev. **103**, 3835 (2003). doi:10.1021/cr0203490
7. G. Wakefield, E. Holland, P.J. Dobson, J.L. Hutchison, Adv. Mater. **13**, 1557 (2001). doi:10.1002/1521-4095(200110)13:20<1557::AID-ADMA1557>3.0.CO;2-W
8. K.L. Frindell, M.H. Bartl, A. Popitsch, G.D. Stucky, Angew. Chem. Int. Ed. **41**, 959 (2002). doi:10.1002/1521-3773(20020315)41:6<959::AID-ANIE959>3.0.CO;2-M
9. L.Y. Wang, Y.D. Li, Nano. Lett. **6**, 1645 (2006). doi:10.1021/nl060684u
10. S.L. Jones, D. Kumar, R.K. Singh, P.H. Holloway, Appl. Phys. Lett. **71**, 404 (1997). doi:10.1063/1.119551
11. K.G. Cho, D. Kumar, P.H. Holloway, R.K. Singh, Appl. Phys. Lett. **73**, 3058 (1998). doi:10.1063/1.122671
12. H. Wang, C.K. Lin, X.M. Liu, J. Lin, M. Yu, Appl. Phys. Lett. **87**, 181907 (2005). doi:10.1063/1.2123382
13. R. Palomino-Merino, A. Conde-Gallardo, M. García-Rocha, I. Hernández-Calderón, V. Castaño, R. Rodríguez, Thin Solid Films **401**, 118 (2001). doi:10.1016/S0040-6090(01)01608-X
14. J.B. Yin, L.Q. Xiang, X.P. Zhao, Appl. Phys. Lett. **90**, 113112 (2007). doi:10.1063/1.2712495
15. Q.G. Zeng, Z.M. Zhang, Z.J. Ding, Y. Wang, Y.Q. Sheng, Scr. Mater. **57**, 897 (2007). doi:10.1016/j.scriptamat.2007.07.027
16. L. Li, C.K. Tsung, Z. Yang, G.D. Stucky, L.D. Sun, J.F. Wang, C.H. Yan, Adv. Mater. **20**, 903 (2008). doi:10.1002/adma.200701507
17. X. Chen, S.S. Mao, Chem. Rev. **107**, 2891 (2007). doi:10.1021/cr0500535
18. H. Bénard, Rev. Gen. Sci. Pures Appl. **11**, 1261 (1900)
19. M. Block, Nature **178**, 650 (1956). doi:10.1038/178650a0
20. J.R.A. Pearson, J. Fluid Mech. **4**, 489 (1958). doi:10.1017/S0022112058000616
21. Y. Lei, L.D. Zhang, G.W. Meng, G.H. Li, X.Y. Zhang, C.H. Liang, W. Chen, S.X. Wang, Appl. Phys. Lett. **78**, 1125 (2001). doi:10.1063/1.1350959
22. K.L. Frindell, M.H. Bartl, M.R. Robinson, G.C. Bazan, A. Popitsch, G.D. Stucky, J. Solid State Chem. **172**, 81 (2003). doi:10.1016/S0022-4596(02)00126-3
23. D.H. Kim, S.H. Kim, K. Lavery, T.P. Russell, Nano. Lett. **4**, 1841 (2004). doi:10.1021/nl049063w